Rehabilitation restores cortical activation profiles and stabilizes synaptic contacts after stroke

Anna Letizia Allegra Mascaro[1,2], Emilia Conti[2], Stefano Lai[3], Antonino Paolo Di Giovanna[2], Cristina Spalletti[1], Claudia Alia[4], Eros Quarta[2], Alessandro Panarese[3], Leonardo Sacconi[2,5], Silvestro Micera[3,6], Matteo Caleo[1], Francesco Saverio Pavone[2,5,7]*

1 Neuroscience Institute, National Research Council, Pisa, Italy,
2 European Laboratory for Non-linear Spectroscopy University of Florence, Italy
3 Scuola Superiore Sant'Anna, Pisa, Italy,
4 Scuola Normale Superiore, Pisa, Italy
5 National Institute of Optics, National Research Council, Italy
6 Ecole Polytechnique Federale de Lausanne (EPFL), Lausanne, Switzerland
7 Department of Physics and Astronomy, University of Florence, Italy

Abstract

Neuro-rehabilitative therapy is the most effective treatment for recovering motor deficits in stroke patients. Nevertheless, the neural basis of recovery associated with rehabilitative intervention is debated. Here, we addressed the multiple facets of cortical remodeling induced by rehabilitative therapy. By longitudinal imaging of cortical activity while training, we demonstrated progressive attenuation of motor map dedifferentiation and rise of a more intense and fast-rising calcium response in the peri-infarct area during movement execution. Coupling of the spared cortex to the injured hemisphere was reinforced by rehabilitation, as demonstrated by our all-optical approach. Alongside, profound angiogenic response accompanied the stabilization of peri-infarct micro-circuitry at the synaptic level. The present work, by combining optical tools of visualization and manipulation of neuronal activity, provides the first *in vivo* evidence of the mechanism of rehabilitation in shaping cortical plasticity.

Introduction

Every year, several millions stroke victims worldwide are impaired by long-term disability implying a large personal and societal burden in lost productivity, lost independence and social withdrawal[1]. Stroke survivors are susceptible to suffer from lifelong losses in sensory, motor, cognitive, and emotional functioning, depending on the size and localization of the lesion. Focal cortical stroke is the leading cause of persistent motor deficits, only somewhat recovered by the limited degree of spontaneous brain repair (see for example Carmichael et al., 2016[2]). Strategies that promote brain plasticity can enhance rewiring and dramatically improve functional outcome. Motor training after ischemic injury is most effective for restoring behavioral performance and peri-infarct neurophysiological maps[3]. Enhanced neuroanatomical changes associated with rehabilitation involve neuronal, glial, and vascular elements of ipsi- and contralesional hemisphere[4, 5]. A number of arm and hand robots have been recently developed to allow intense training without costly physiotherapy assistance while ensuring repeatable training and objective measures of motor performance[6, 7]. Nevertheless, the lack of complete neuronal repair and the limitation of functional recovery attained by motor training led researchers to consider joint strategies[8]. Neuro-rehabilitative research is now developing novel treatments to maximize the effectiveness of rehabilitative therapies through a combination of physical therapy and other plasticizing treatment like cortical stimulation or pharmacological intervention[9-12]. The synergic action of these paired protocols proved to be effective

in determining a generalized improvement of motor skills in the post-acute phase after stroke[13, 14]. Many of these treatments exploit modulation of contralesional hemisphere activity to counteract disruptive influences of the intact hemisphere on the injured one (see, for example Wang et al., 2012[15]). The interference is often linked with worsened behavioral outcome in stroke patients[16, 17]. Unfortunately, clinical studies using transcranial magnetic stimulation (TMS) or transcranial direct current stimulation (tDCS) aiming at modulating neuronal connectivity by inhibiting the contralesional hemisphere led to contradictory results, showing in some cases the efficacy and in others the drawbacks of this approach[18-26]. This ambiguity emphasizes that our current understanding of the mechanism of large- and small-scale rewiring after stroke, modulated by ad hoc treatment, are at best incomplete.

A recent study (Spalletti et al., submitted) showed that the combination of motor training and pharmacological inhibition of the contralesional primary motor cortex (M1) is responsible for a generalized recovery of motor skills. Importantly, the motor improvement is not task-specific while being generalized to other motor functions, as reflected by several kinematic parameters in multiple behavioral tests. Here, we dissected how this rehabilitative treatment molded cortical plasticity by first getting the big picture of large-scale cortical remapping on the lesioned and healthy hemisphere, and then digging into the finer synaptic details. To address large and small scales we took advantage of selected optical imaging and manipulation techniques *in vivo*. In detail, by longitudinal imaging of cortical functionality in awake GCaMP6f mice with wide-field fluorescence microscopy we dissected large-scale remapping of the injured hemisphere. We then investigated how the inter-hemispheric connectivity is affected by using an all-optical approach via optogenetic stimulation of the homotopic area in the contralateral cortex. Vascular maps are generated by two-photon fluorescence microscopy (TPFM) of cleared brain samples to address aspects of neurovascular coupling after stroke. Finally, the stabilizing effect of rehabilitation on synaptic plasticity is monitored by longitudinal TPFM on GFPM mice *in vivo*.

Results

Combined rehabilitation treatment recapitulates the dedifferentiation induced by stroke

We took advantage of a rehabilitation protocol that combines highly repeatable training of the mouse forelimb in a robotic platform (M-Platform[27]) with reversible inactivation of the healthy, contralesional hemisphere via BoNT/E. The injection of the toxin transiently counterbalanced the early increase of activity in the contralesional hemisphere (Supplementary Fig. 1A). Rehabilitation-associated training consisted in repeated cycles of triggered extension followed by active retraction of the contralesional forelimb on the M-Platform (Fig. 1A and Supplementary Fig. 1B). REHAB mice were trained for 4 weeks starting 5 days after photothrombotic stroke was performed on right M1, in line with the overall consensus that initiating rehabilitative training 5 or more days after stroke is mostly beneficial and has no adverse effects[28] (Supplementary Fig. 1C). The motor task was rapidly learned and easily performed from the earliest sessions after stroke. The treatment induced a substantial improvement of motor performances, as assessed by the Schallert Cylinder test one month after the lesion. Indeed, the asymmetry in forelimb use induced by stroke was no longer present in treated mice (Supplementary Fig. 1D). To assess to what extent the motor performance was accompanied by plastic rearrangements

of cortical networks at different scales, we investigated the remapping of motor representations, the vascular network remodeling and the synaptic dynamics.

Our idea was to evaluate first how rehabilitation modulate cortical plasticity of photothrombotic stroke mice in vivo. We thus implemented an integrated system for simultaneous meso-scale calcium imaging of cortical activity on GCaMP6f mice and recording of forces applied by the contralesional forelimb during the training sessions on the M-Platform (Fig. 1A-C).

As previously reported, motor-targeted focal stroke molds motor maps towards an abnormally scattered or diffuse structure that persists more than a month after stroke (see for example Harrison et al. 2013[29]). Accordingly, wide-field imaging shows that a large area covering most of the cortical surface of the injured hemisphere lights up synchronously during the retraction movement in non-treated mice 4 weeks after stroke. Remarkably, rehabilitation re-established a pattern of activation similar to healthy controls (Fig 1D, Supplementary Fig. 2A). By overlapping the retraction-triggered cortical maps obtained on every day of the training week, we quantified the spatial extent and source of activation of the calcium waves (Supplementary Fig. 2B-D). Stroke shifted the focus and doubled the extension of the motor representation towards other regions not specifically associated with motor control (Supplementary Fig. 2C, middle panel). The pattern of clustered activation is substantially recovered in terms of extension and focus in the rehabilitated group (Supplementary Fig. 2C-D). The reduced spread of cortical activation positively correlates with the proximity to the lesion in REHAB mice (Supplementary Fig. 2D). In few cases, the focusing was associated with increased functional connectivity between the primary motor output and secondary motor areas (Supplementary Fig. 2E). Our results indicate that the combined rehabilitative treatment focalizes the cortical activation to the peri-infarct region while limiting the concurrent recruiting of distant locations. We wondered whether the spatial spread of calcium waves implied a synchronicity in activation of peri-infarct network and distal inter-connected region. By analyzing the temporal profile of motor task-triggered cortical activation, we found that the delay between the maximum of calcium peak of rostral and caudal regions was reversed in the stroke group compared to healthy mice, meaning that the caudal region anticipated the peri-infarct areas (Fig. 1E). Longitudinal imaging shows a progressive recovery of the average calcium activation dynamics during the 4 weeks of training (Supplementary Fig. 2F, left panel). The longer lag in REHAB group closely resembles the spatio-temporal profile of healthy animals, confirming that the motor output primarily involves the peri-infarct region. Here, we found that the combined treatment profoundly affected the neuronal activation patterns. The average traces in Fig. 1F show at a glance the substantial differences in the calcium dynamic measured in the region of maximum activation during movement production. From the curves, while significant reduction in the amplitude of the cortical activity during the motor output was evident one month after stroke, high affinity is evinced on the activation kinetics of REHAB and non-injured mice. Four weeks of training allowed progressive recovery of the amplitude of the calcium response (Fig. 1G and Supplementary Fig. 2F, middle panel). The augmented activation of the neuronal population deputed to motor command could be correlated to a more efficient and fast recruitment. Indeed, treated animals show a progressive increase in the slope of calcium activation during the rehabilitation period (Supplementary Fig. 2F, right panel). REHAB mice build a consistently faster activation curve during the motor task after 4 weeks of training (Fig. 1H). In conclusion, by performing longitudinal analysis of cortical functionality, we show that rehabilitative treatment promotes the recovery of the temporal and spatial features of the cortical activation patterns associated with motor execution in the peri-infarct region. After analyzing the

ipsilateral modulation of activity, we guessed how distal interconnected regions like the contralesional motor cortex were affected by our therapeutic intervention.

All-optical investigation reveals rehabilitation-induced tightening of inter-hemispheric effective connectivity

The debate on the support function of the contralesional cortex on the motor recovery is still open. Several studies on mice and humans showed that interhemispheric M1 connectivity is reduced after stroke[30-32]. Increased connectivity is hypothesized to positively correlate with recovery of motor performance at the subacute stage after stroke in humans[33]. Along with this hypothesis, we tested whether the interhemispheric connectivity between homotopic areas of the two hemispheres was modulated by rehabilitation. To this purpose, we used an all-optical approach that combines optogenetic activation of the intact M1 with recording of calcium-related activation in the injured hemisphere. In this experiments, the left M1s of GCaMP6f mice were injected with AAV9-CaMKII-ChR2-mCherry (Fig. 2A). One month after stroke, we performed optogenetic stimulation of spared M1. In order to avoid cross talk between GCaMP6f and ChR2 stimulation, we modified the wide-field microscope by partially occluding the 505 nm LED (Fig. 2B-C). Optogenetic stimulation was realized by taking advantage of a second excitation path where a 470 nm laser was focalized on the AAV-transfected region via acousto-optic deflectors (AODs). Laser irradiation of the contralesional M1 could reproducibly trigger the spreading of calcium waves in the injured hemisphere (Fig. 2D, Supplementary Video 1). The light-stimulation mainly recruited the homotopic M1 in CTRL mice and peri-infarct area in injured animals (Supplementary Fig. 2). Afterwards, it propagated to functionally connected regions, located either anterior or posterior to the primary source of activation (Supplementary Video 1). At a glance, the calcium waves' temporal dynamics was comparable between healthy and STROKE mice (Supplementary Fig. 2). Indeed, by quantifying the delay in contralesional response of optogenetically-triggered calcium responses, we found no significant difference between STROKE and CTRL mice, suggesting that some form of spontaneous recovery compensated the reduced interhemispheric connectivity caused by the lesion (Fig. 2E). On the contrary, the delay between the delivery of the illumination stimulus and the functional response on the injured hemisphere was significantly reduced in treated mice. Accordingly, the success rate of contralateral stimulation was higher after 4 weeks of training (Fig. 2F). Therefore, by using an all-optical investigation we highlighted how rehabilitation strengthened the functional connectivity between the spared motor and the perilesional cortex. We then wondered if the functional remapping at the local and inter-hemispheric level had a structural correlate of vascular reorganization.

Rehabilitative treatment promotes angiogenesis in the peri-infarct area

Vascular remodeling and angiogenesis, known to occur after stroke, correlate with improved functional outcome, and can be augmented by targeted therapies[34]. Previous neuroimaging studies[35] showed how the formation of new blood vessels (BV) improved the exchange of oxygen and glucose in hypoxic tissue, and subsequent functional outcomes by increasing the blood flow in affected region[36-38]. Thus, fostering angiogenesis is an effective strategy for treatments of stroke[39]. We wondered how rehabilitation molds structural features of vasculature networks.

In the days following the insult, the injured area consistently shrunk due to the collapse of dead tissue, as observed in longitudinally imaged mouse cortices under both the cranial window and thinned skull preparation (Fig. 3A). In addition, a very bright spot appeared in the peri-infarct region of GCaMP6 mice,

possibly resembling the excitotoxic response elicited by the photothrombotic stroke (see, for example, left panel of Fig. 3A; 13 out of 14 injured mice). The enhanced brightness gradually diminished and disappeared after the acute period (6-19 days after stroke), along with a massive shrinkage of the necrotic tissue. The consequent displacement of the peri-infarct area was associated with substantial remodeling of blood vessels, in agreement with previous studies[40]. In order to quantify this structural reshaping, we performed 3D reconstructions of cortical vasculature. In detail, after the last motor training session we and stained the brain vasculature of GFPM mice with a vessel-filling fluorescent dye, albumin-FITC (Fig. 3B). By performing TPFM on TDE-cleared cortical slices (see Methods), we obtained high-resolution 3D maps of blood vessels of the injured hemisphere (Fig. 3C, Supplementary Video 2). We found that the blood vessel orientation of REHAB mice was similar to the STROKE group (Fig. 3D-E). Indeed, combined treatment did not rescue random vascular orientation nor in proximal (<500 µm) or distal (1000 to 1500 µm from core) regions. On the other hand, the density of blood vessels near the infarct site is significantly higher in treated mice (Fig. 3F, left panel). We further evaluated the density profile over the entire cortical depth, to define the layer-specific contribution in the increased BV density. BV distribution was uniform both in healthy and injured non-treated mice. Increases in density localized mainly in the middle and deeper layer of the cortex (300-700 µm deep) in REHAB group (Fig. 3F, middle panel). We found that this inhomogeneity, possibly due to treatment-induced angiogenesis, mainly involves region proximal to the stroke core (Fig. 3F right panel). In conclusion, by combining *in vivo* and *ex vivo* imaging methods we realized 3D vascular maps and dissected the proangiogenic effect of the rehabilitative treatment on the peri-infarct and distal vasculature. In parallel with vascular reshaping, we explored the possible contribution of finer neuro-anatomical adaptations to define their contribution to the remapping of functional representations onto new brain locations after stroke.

Rehabilitation promotes the stabilization of synaptic microcircuits in the peri-infarct area

Heightened structural remodeling has been observed in both presynaptic (axonal fibers and terminals) and postsynaptic (dendrites and dendritic spines) neuronal structures in peri-infarct cortex in the weeks following stroke[41-45]. Tissue migration and rearrangement over several hundredths of microns caused by the collapse of dead tissue in the stroke core profoundly alter the microcircuitry at the synaptic level[40]. According to the hypothesis that rehabilitation is associated with profound alteration of cortical circuits at the synaptic level[46], we performed TPFM of pyramidal apical dendrites (up to 100 µm deep from pial surface) at increasing distances (up to 4 mm) from the stroke core on GFPM mice. The imaging area overlaps with the region visualized in GCaMP6f mice experiments (Supplementary Fig. 4A). We show that in the same animals the migration of tissue (Fig. 4A, left panels) that led to a considerable re-orientation of blood vessels after stroke produced analogous reshaping on cortical dendrites and axons in the peri-infarct area (Fig. 4A, right panels). On the contrary, alignment of pyramidal processes was not visible in treated animals even if stroke profoundly altered the distribution of blood vessels around the core (Fig. 4B; same animals as in blood vessel analysis). Indeed, the randomness in dendrite orientation was partially restored in REHAB mice. Reorientation was less pronounced in both treated and non-treated animals with increasing distance from the ischemic core (>1 mm; Supplementary Fig. 4C).

Ischemic damage-induced alterations of the microcircuitry are known to impinge on dendrites as well as synaptic contacts, producing massive increase of spine turnover in the peri-infarct area[40, 47]. We evaluated how the synaptic plasticity was modulated by the rehabilitative treatment by monitoring the appearance and disappearance of apical dendritic spines (Fig. 4C). We thus performed a frame-by-frame comparison of spines in the mosaic we acquired along the rostro-caudal axis with TPFM. From

this analysis, we derived the Surviving Fraction (SF), the Turnover Ratio (TOR) and the spine Density (D). Spines in the remapped peri-infarct region selectively exhibited increased synaptic stability (Fig. 4D, left panel) and a lower turnover (Fig. 4D, middle panel). The treatment reinstated higher synaptic densities in the stabilized circuits, comparable to pre-stroke values (Fig. 4D, right panel). Consistent with previously shown results on dendrites and blood vessels, rehabilitation intervention on cortical rewiring was stronger at the proximal level, and weakened with increasing distance from the ischemic core (Supplementary Fig. 4D). In brief, longitudinal imaging of cortical neurons revealed how the rehabilitative therapy tweaked the synaptic equilibrium to control levels, consistently with the lighter alterations in spatial orientation of pyramidal dendrites.

Discussion

In the present study, we addressed ad hoc optical imaging and manipulation techniques to get the coarse-grained picture of rehabilitation-induced cortical remodeling on the lesioned and healthy hemisphere, and then disclose synaptic particulars. We show that our rehabilitative treatment stabilized the peri-lesional synaptic contacts while refining the neuronal population deputed to motor control, and promoted the formation of an enriched vascular environment for feeding the neurons newly activated to this purpose. To the best of our knowledge, our results provide the first evidence of the correlation of rehabilitation-induced cortical and vascular reshaping via longitudinal *in vivo* imaging.

The functional reorganization of ensemble neuronal activities was observed while stroke mice performed motor training on the M-Platform, thus allowing correlation of the applied forces and the cortical motor command. The diffuse structure of motor maps we observed in post-acute stroke, previously shown by Harrison et al.[29], is supposed to represent the ongoing reorganization of the underlying cortical circuitry. In agreement with this study, the new motor map could emerge from a population of sensory neurons progressively shifting their role towards motor control (see Matyas et al.[48] and Supplementary Fig. 1D). Rehabilitation re-establishes a clustering of neuronal population activity deputed to motor, reinstating functional parameters that highly resemble healthy conditions. The massive plastic reshaping of cortical representations taking place in the subacute phase after stroke might be linked to increased integrity of cortico-spinal fibers[49, 50] or myelination of transcallosal fibres[50].

By performing optogenetic stimulation on the same mice, we demonstrate that progressive focusing of motor control in the ipsilesional cortex is associated with increased interhemispheric coupling. The connectivity between homotopic motor cortices, reduced after the lesion, might be readdressed by vicariant neurons to the peri-infarct area via massive structural rearrangement. Our results suggest a possible correlation between the refinement of the neuronal population in the perilesional area controlling motor outputs and the reinforcement of connectivity of pyramidal neurons projecting from the healthy M1. Refocusing could be supported by the activity of contralesional pyramidal cells projecting to sensory neurons in the peri-infarct area. The new functional pathway probably derives from axons spared by the lesion or from newly sprouted branches[2]. Other studies previously combined voltage sensitive dyes with optogenetic actuators to enquire cortical functional connectivity[51, 52]. Recently, this approach has been applied to stroke models, showing a spontaneous partial recovery of functional connectivity 8 weeks after injury[53]. Our model that combines transgenic GCaMP6 mice with AAV-induced expression of ChR2 in the homotopic M1 has the advantage of stable control and monitoring of neuronal activity over weeks and months. We anticipate that the all-optical approach we

used will be further extended to the longitudinal exploration of the bidirectional inter-hemispheric connectivity.

The improvement in brain function after stroke is often associated with an angiogenic response. Indeed, a close relation exists between the proangiogenic state and the neurological improvement in patients with stroke[54-56]. The region of active neovascularization acts as a niche for enhanced neuronal remodeling[57, 58], thus suggesting a direct link between angiogenesis and tissue repair. Although the formation of new blood vessel in the ischemic area may be transient, enduring recovery might result from the association of angiogenesis with neuronal plasticity[59]. We reasoned that circuit reshaping and refinement we observe in rehabilitated mice might be aided by angiogenesis and vascularization. An improved neurovascular coupling could be linked to a higher efficiency of neuronal enrolment in the peri-infarct region revealed in our study by the clustering of the motor output. Based on our results, we hypothesize that the transient "proangiogenic state" induced in response to ischemic insult is consolidated and further promoted by rehabilitation. We forecast that we will further extend the study on vasculature remapping induced by rehabilitation after stroke by performing light-sheet imaging of the entire mouse brain[60-62].

The genesis of this enriched milieu around the infarct area supplied with fresh nourishment promotes, in addition to axonal sprouting, synaptogenesis and dendritic remodeling[41, 63, 64]. The pro-plastic environment counteracts the loss of neurons and synaptic contacts in the core of ischemic injury by promoting the rewiring of dendrites and axons in the injured region. Previous postmortem histological studies on stroke-induced structural plasticity highlighted the transient decline and following recovery in synaptic densities around the infarct[65, 66]. Rehabilitative training might shape the spared and the new circuits by selecting and stabilizing the active contacts and pruning of the non-functional ones[14]. Rehabilitation was reported to significantly enhance both dendritic architecture and spine number in the perilesional area[46]. Nevertheless, a shortcoming of *ex vivo* studies is that they provide only endpoint measures of reorganization, while dynamic aspects of dendritic remodeling could not be evaluated[67]. On the other hand, *in vivo* imaging offers a unique insight into how neurons in the intact nervous system are altered by pathology[67]. The high resolution of TPFM has been used to longitudinally evaluate *in vivo* synaptic plasticity after stroke [68]. *In vivo* imaging showed that the extent of recovery varies along the distance from the infarct core[69]. Another longitudinal *in vivo* study founds evidence for redistributions of blood vessel and dendrite orientation confined to the regions near the infarct border few weeks after photothrombotic stroke[40]. To our knowledge, no *in vivo* investigation reported yet on how rehabilitation acted on synaptic turnover. In the present study, we longitudinally evaluated large-scale dendritic and axonal reorientation determined by our rehabilitative treatment. Similar to previous *in vivo* experiments, we saw that the collapse of dead tissue created, in the same animals, a strong orientation gradient both of blood vessels and neurites towards the ischemic core. We show for the first time that rehabilitation is sufficient to endorse the recovery of structural features characteristics of healthy neuronal network. The restorative therapy partially rescued the random orientation at the micro-circuitry level and supported the stabilization of synaptic contacts. Indeed, rehabilitation counterbalanced the increased synaptic turnover induced by stroke by reinstating pre-lesion dynamics. Our multi-scale investigation brought to light complementary aspects of the structural and functional plasticity induced by rehabilitation that may lay the ground to the development of more efficient therapies.

Acknowledgements

This project has received funding from the H2020 EXCELLENT SCIENCE - European Research Council (ERC) under grant agreement ID n. 692943 BrainBIT". In addition, it was supported by the European Union's Horizon 2020 research and innovation programme under grant agreements No. 720270 (Human Brain Project) and 654148 (Laserlab-Europe). The project have also been supported by the Italian Ministry for Education, University, and Research in the framework of the Flagship Project NanoMAX, and by "Ente Cassa di Risparmio di Firenze" (private foundation). Part of this work was performed in the frame of the Proof of Concept Studies for the ESFRI research infrastructure project Euro-BioImaging at the PCS facility LENS.

Bibliography

1. Mozaffarian, D.*, et al.* Heart disease and stroke statistics--2015 update: a report from the American Heart Association. *Circulation* **131**, e29-322 (2015).
2. Carmichael, S.T., Kathirvelu, B., Schweppe, C.A. & Nie, E.H. Molecular, cellular and functional events in axonal sprouting after stroke. *Experimental neurology* **287**, 384-394 (2017).
3. Jones, T.A. & Adkins, D.L. Motor System Reorganization After Stroke: Stimulating and Training Toward Perfection. *Physiology* **30**, 358-370 (2015).
4. Biernaskie, J., Chernenko, G. & Corbett, D. Efficacy of rehabilitative experience declines with time after focal ischemic brain injury. *The Journal of neuroscience : the official journal of the Society for Neuroscience* **24**, 1245-1254 (2004).
5. Cumberland Consensus Working, G.*, et al.* The future of restorative neurosciences in stroke: driving the translational research pipeline from basic science to rehabilitation of people after stroke. *Neurorehabilitation and neural repair* **23**, 97-107 (2009).
6. Veerbeek, J.M., Langbroek-Amersfoort, A.C., Wegen, E.E.H.v., Meskers, C.G.M. & Kwakkel, G. Effects of Robot-Assisted Therapy for the Upper Limb After Stroke. *Neurorehabilitation and neural repair* **31**, 107-121 (2017).
7. Lo, K., Stephenson, M. & Lockwood, C. Effectiveness of robotic assisted rehabilitation for mobility and functional ability in adult stroke patients: a systematic review protocol. *JBI Database of Systematic Reviews and Implementation Reports* **15**, 39-48 (2017).
8. Di Pino, G.*, et al.* Modulation of brain plasticity in stroke: a novel model for neurorehabilitation. *Nature reviews. Neurology* **10**, 597-608 (2014).
9. Dancause, N. & Nudo, R.J. Shaping plasticity to enhance recovery after injury. *Progress in brain research* **192**, 273-295 (2011).
10. Plautz, E.J.*, et al.* Post-infarct cortical plasticity and behavioral recovery using concurrent cortical stimulation and rehabilitative training: a feasibility study in primates. *Neurological research* **25**, 801-810 (2003).
11. Adkins-Muir, D.L. & Jones, T.A. Cortical electrical stimulation combined with rehabilitative training: enhanced functional recovery and dendritic plasticity following focal cortical ischemia in rats. *Neurological research* **25**, 780-788 (2003).
12. Hesse, S.*, et al.* Combined transcranial direct current stimulation and robot-assisted arm training in subacute stroke patients: a pilot study. *Restorative neurology and neuroscience* **25**, 9-15 (2007).
13. Frost, S.B., Barbay, S., Friel, K.M., Plautz, E.J. & Nudo, R.J. Reorganization of remote cortical regions after ischemic brain injury: a potential substrate for stroke recovery. *Journal of neurophysiology* **89**, 3205-3214 (2003).
14. Wahl, A.S.*, et al.* Neuronal repair. Asynchronous therapy restores motor control by rewiring of the rat corticospinal tract after stroke. *Science* **344**, 1250-1255 (2014).

15. Wang, R.Y., *et al.* rTMS combined with task-oriented training to improve symmetry of interhemispheric corticomotor excitability and gait performance after stroke: a randomized trial. *Neurorehabilitation and neural repair* **26**, 222-230 (2012).
16. Ward, N.S. & Cohen, L.G. Mechanisms underlying recovery of motor function after stroke. *Archives of neurology* **61**, 1844-1848 (2004).
17. Grefkes, C. & Fink, G.R. Reorganization of cerebral networks after stroke: new insights from neuroimaging with connectivity approaches. *Brain : a journal of neurology* **134**, 1264-1276 (2011).
18. Fregni, F., *et al.* A sham-controlled trial of a 5-day course of repetitive transcranial magnetic stimulation of the unaffected hemisphere in stroke patients. *Stroke* **37**, 2115-2122 (2006).
19. Khedr, E.M., Rothwell, J.C. & El-Atar, A. One-year follow up of patients with chronic tinnitus treated with left temporoparietal rTMS. *European journal of neurology* **16**, 404-408 (2009).
20. Mansur, C.G., *et al.* A sham stimulation-controlled trial of rTMS of the unaffected hemisphere in stroke patients. *Neurology* **64**, 1802-1804 (2005).
21. Nowak, D.A., *et al.* Effects of low-frequency repetitive transcranial magnetic stimulation of the contralesional primary motor cortex on movement kinematics and neural activity in subcortical stroke. *Archives of neurology* **65**, 741-747 (2008).
22. Maeda, F., Gangitano, M., Thall, M. & Pascual-Leone, A. Inter- and intra-individual variability of paired-pulse curves with transcranial magnetic stimulation (TMS). *Clinical neurophysiology : official journal of the International Federation of Clinical Neurophysiology* **113**, 376-382 (2002).
23. Takeuchi, N., Chuma, T., Matsuo, Y., Watanabe, I. & Ikoma, K. Repetitive transcranial magnetic stimulation of contralesional primary motor cortex improves hand function after stroke. *Stroke* **36**, 2681-2686 (2005).
24. Biernaskie, J., Szymanska, A., Windle, V. & Corbett, D. Bi-hemispheric contribution to functional motor recovery of the affected forelimb following focal ischemic brain injury in rats. *The European journal of neuroscience* **21**, 989-999 (2005).
25. Lotze, M., *et al.* The role of multiple contralesional motor areas for complex hand movements after internal capsular lesion. *The Journal of neuroscience : the official journal of the Society for Neuroscience* **26**, 6096-6102 (2006).
26. Di Lazzaro, V., *et al.* Modulating cortical excitability in acute stroke: a repetitive TMS study. *Clinical neurophysiology : official journal of the International Federation of Clinical Neurophysiology* **119**, 715-723 (2008).
27. Spalletti, C., *et al.* A robotic system for quantitative assessment and poststroke training of forelimb retraction in mice. *Neurorehabilitation and neural repair* **28**, 188-196 (2014).
28. Krakauer, J.W., Carmichael, S.T., Corbett, D. & Wittenberg, G.F. Getting neurorehabilitation right: what can be learned from animal models? *Neurorehabilitation and neural repair* **26**, 923-931 (2012).
29. Harrison, T.C., Silasi, G., Boyd, J.D. & Murphy, T.H. Displacement of sensory maps and disorganization of motor cortex after targeted stroke in mice. *Stroke* **44**, 2300-2306 (2013).
30. van Meer, M.P., *et al.* Recovery of sensorimotor function after experimental stroke correlates with restoration of resting-state interhemispheric functional connectivity. *The Journal of neuroscience : the official journal of the Society for Neuroscience* **30**, 3964-3972 (2010).
31. van Meer, M.P., van der Marel, K., Otte, W.M., Berkelbach van der Sprenkel, J.W. & Dijkhuizen, R.M. Correspondence between altered functional and structural connectivity in the contralesional sensorimotor cortex after unilateral stroke in rats: a combined resting-state functional MRI and manganese-enhanced MRI study. *Journal of cerebral blood flow and metabolism : official journal of the International Society of Cerebral Blood Flow and Metabolism* **30**, 1707-1711 (2010).
32. Bauer, A.Q., *et al.* Optical imaging of disrupted functional connectivity following ischemic stroke in mice. *NeuroImage* **99**, 388-401 (2014).
33. Carter, A.R., *et al.* Resting interhemispheric functional magnetic resonance imaging connectivity predicts performance after stroke. *Annals of neurology* **67**, 365-375 (2010).

34. Ergul, A., Alhusban, A. & Fagan, S. Angiogenesis: a harmonized target for recovery after stroke. *Stroke; a journal of cerebral circulation* **43**, 2270-2274 (2012).
35. Jiang, Q.*, et al.* Investigation of neural progenitor cell induced angiogenesis after embolic stroke in rat using MRI. *NeuroImage* **28**, 698-707 (2005).
36. Arai, K., Jin, G., Navaratna, D. & Lo, E.H. Brain angiogenesis in developmental and pathological processes: neurovascular injury and angiogenic recovery after stroke. *FEBS journal* **276**, 4644-4652 (2009).
37. Favier, J. & Corvol, P. Physiological angiogenesis. *Therapie* **56**, 455-463 (2000).
38. Hayashi, T.*, et al.* Cerebral ischemia and angiogenesis. *Current neurovascular research* **3**, 119-129 (2006).
39. Zhang, P.*, et al.* Early exercise improves cerebral blood flow through increased angiogenesis in experimental stroke rat model. *Journal of NeuroEngineering and Rehabilitation* **10**, 43 (2013).
40. Brown, C.E., Li, P., Boyd, J.D., Delaney, K.R. & Murphy, T.H. Extensive turnover of dendritic spines and vascular remodeling in cortical tissues recovering from stroke. *The Journal of neuroscience : the official journal of the Society for Neuroscience* **27**, 4101-4109 (2007).
41. Brown, C.E., Boyd, J.D. & Murphy, T.H. Longitudinal in vivo imaging reveals balanced and branch-specific remodeling of mature cortical pyramidal dendritic arbors after stroke. *Journal of cerebral blood flow and metabolism : official journal of the International Society of Cerebral Blood Flow and Metabolism* **30**, 783-791 (2010).
42. Carmichael, S.T., Wei, L., Rovainen, C.M. & Woolsey, T.A. New patterns of intracortical projections after focal cortical stroke. *Neurobiology of disease* **8**, 910-922 (2001).
43. Hsu, J.E. & Jones, T.A. Contralesional neural plasticity and functional changes in the less-affected forelimb after large and small cortical infarcts in rats. *Experimental neurology* **201**, 479-494 (2006).
44. Ueno, Y.*, et al.* Axonal outgrowth and dendritic plasticity in the cortical peri-infarct area after experimental stroke. *Stroke* **43**, 2221-2228 (2012).
45. Dancause, N.*, et al.* Extensive cortical rewiring after brain injury. *The Journal of neuroscience : the official journal of the Society for Neuroscience* **25**, 10167-10179 (2005).
46. Wang, L., Conner, J.M., Nagahara, A.H. & Tuszynski, M.H. Rehabilitation drives enhancement of neuronal structure in functionally relevant neuronal subsets. *Proceedings of the National Academy of Sciences* **113**, 2750-2755 (2016).
47. Mostany, R.*, et al.* Local hemodynamics dictate long-term dendritic plasticity in peri-infarct cortex. *The Journal of neuroscience : the official journal of the Society for Neuroscience* **30**, 14116-14126 (2010).
48. Matyas, F.*, et al.* Motor control by sensory cortex. *Science* **330**, 1240-1243 (2010).
49. Carter, A.R.*, et al.* Upstream dysfunction of somatomotor functional connectivity after corticospinal damage in stroke. *Neurorehabilitation and neural repair* **26**, 7-19 (2012).
50. van Meer, M.P.*, et al.* Extent of bilateral neuronal network reorganization and functional recovery in relation to stroke severity. *The Journal of neuroscience : the official journal of the Society for Neuroscience* **32**, 4495-4507 (2012).
51. Ayling, O.G., Harrison, T.C., Boyd, J.D., Goroshkov, A. & Murphy, T.H. Automated light-based mapping of motor cortex by photoactivation of channelrhodopsin-2 transgenic mice. *Nature methods* **6**, 219-224 (2009).
52. Lim, D.H., LeDue, J.M. & Murphy, T.H. Network analysis of mesoscale optical recordings to assess regional, functional connectivity. *Neurophotonics* **2**, 041405 (2015).
53. Lim, D.H., LeDue, J.M., Mohajerani, M.H. & Murphy, T.H. Optogenetic mapping after stroke reveals network-wide scaling of functional connections and heterogeneous recovery of the peri-infarct. *The Journal of neuroscience : the official journal of the Society for Neuroscience* **34**, 16455-16466 (2014).

54. Arkuszewski, M., Świat, M. & Opala, G. Perfusion computed tomography in prediction of functional outcome in patients with acute ischaemic stroke. *Nuclear Medicine Review* **12**, 89-94 (2009).
55. Hermann, D.M. & Chopp, M. Promoting brain remodelling and plasticity for stroke recovery: therapeutic promise and potential pitfalls of clinical translation. *The Lancet Neurology* **11**, 369-380 (2012).
56. Xiong, Y., Mahmood, A. & Chopp, M. Angiogenesis, neurogenesis and brain recovery of function following injury. *Curr Opin Invest Dr* **11**, 298-308 (2010).
57. Shen, Q*., et al.* Adult SVZ stem cells lie in a vascular niche: a quantitative analysis of niche cell-cell interactions. *Cell stem cell* **3**, 289-300 (2008).
58. Prakash, R. & Carmichael, S.T. Blood-brain barrier breakdown and neovascularization processes after stroke and traumatic brain injury. *Current opinion in neurology* **28**, 556-564 (2015).
59. Ergul, A., Alhusban, A. & Fagan, S.C. Angiogenesis: A Harmonized Target for Recovery after Stroke. *Stroke* **43**, 2270-2274 (2012).
60. Silvestri, L., Mascaro, A.L.A., Costantini, I., Sacconi, L. & Pavone, F.S. Correlative two-photon and light sheet microscopy. *Methods* **66**, 268-272 (2014).
61. Silvestri, L., Mascaro, A.L.A., Costantini, I., Sacconi, L. & Pavone, F.S. Exploring the brain on multiple scales with correlative two-photon and light sheet microscopy. *Proc Spie* **8948** (2014).
62. Lugo-Hernandez, E*., et al.* 3D visualization and quantification of microvessels in the whole ischemic mouse brain using solvent-based clearing and light sheet microscopy. *Journal of Cerebral Blood Flow & Metabolism* **0**, 0271678X17698970.
63. Kelley, M.S. & Steward, O. Injury-induced physiological events that may modulate gene expression in neurons and glia. *Reviews in the neurosciences* **8**, 147-177 (1997).
64. Carmichael, S.T. Cellular and molecular mechanisms of neural repair after stroke: making waves. *Annals of neurology* **59**, 735-742 (2006).
65. Gonzalez, C.L. & Kolb, B. A comparison of different models of stroke on behaviour and brain morphology. *The European journal of neuroscience* **18**, 1950-1962 (2003).
66. Corbett, D., Giles, T., Evans, S., McLean, J. & Biernaskie, J. Dynamic changes in CA1 dendritic spines associated with ischemic tolerance. *Experimental neurology* **202**, 133-138 (2006).
67. Misgeld, T. & Kerschensteiner, M. In vivo imaging of the diseased nervous system. *Nat Rev Neurosci* **7**, 449-463 (2006).
68. Sakadzic, S., Lee, J., Boas, D.A. & Ayata, C. High-resolution in vivo optical imaging of stroke injury and repair. *Brain research* **1623**, 174-192 (2015).
69. Sigler, A. & Murphy, T.H. In vivo 2-photon imaging of fine structure in the rodent brain: before, during, and after stroke. *Stroke* **41**, S117-123 (2010).

Figure 1

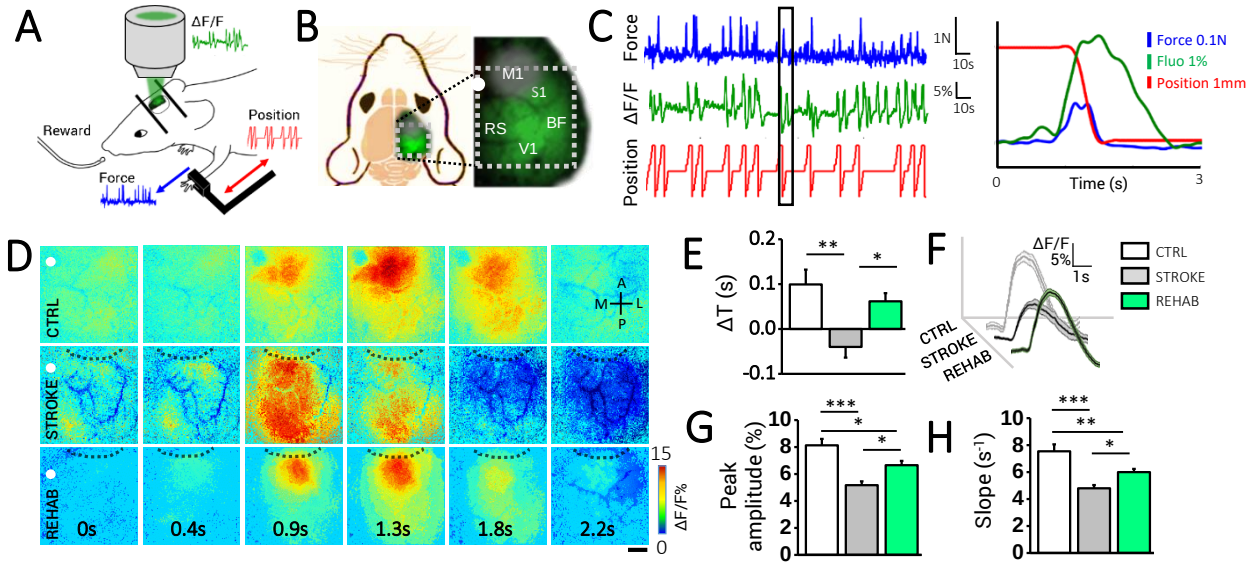

Figure 1: **Rehabilitation refocuses cortical control of motor output and restores activation profiles in the peri-infarct region**. (A) Graphic representation of the M-Platform for rehabilitative training and simultaneous calcium imaging of cortical activity. (B) Schematic representation of field of view (i.e. area within dotted white square) for wide-field imaging on GCaMP6f mice. The grey cloud indicates the location and approximate extension of the lesion. M1, Primary Motor Area; S1, Primary Somatosensory area; BF, Barrel Field; V1, Primary Visual Cortex; RS, RetroSplenial cortex. The white dot indicates bregma. (C) Example of force trace recorded by the load cell during the passive-extension, active-retraction trials on the rehabilitative platform (blue trace), the simultaneously recorded calcium fluorescence trace (green trace) and the position of the slit (red trace). The right graph shows overlapped the simultaneously recorded traces correponding to the black box on the left. (D) Image sequence of cortical activation during pulling of the handle by contralateral forelimb, from 0.4s before to 1.8s after the onset of the force peak. Black dashed lines define lesion borders, white dot indicates bregma. (E) Delays in cortical activation in caudal regions are reported for the 3 groups ($Nmice_{CTRL}$= 4, $Nmice_{STROKE}$ = 6, $Nmice_{REHAB}$= 6; ANOVA One Way followed by Bonferroni Test, *P* (CTRL/STROKE)<0.01, *P* (STROKE/REHAB)<0.05). (F) Average calcium traces for the three experimental groups; the shadows report the SEM. (G) The graph shows the maximum of the fluorescence peaks (ANOVA One Way followed by Bonferroni Test, *P* (CTRL/STROKE)<0.001, *P*(CTRL/REHAB)< 0.05). (H) The graph shows the slope (average ± SEM) of the fluorescence in the rising phase (ANOVA One Way followed by Bonferroni Test, *P* (CTRL/STROKE)<0.001, *P* (STROKE/REHAB)< 0.05, , *P* (CTRL/REHAB)< 0.01).

Figure 2

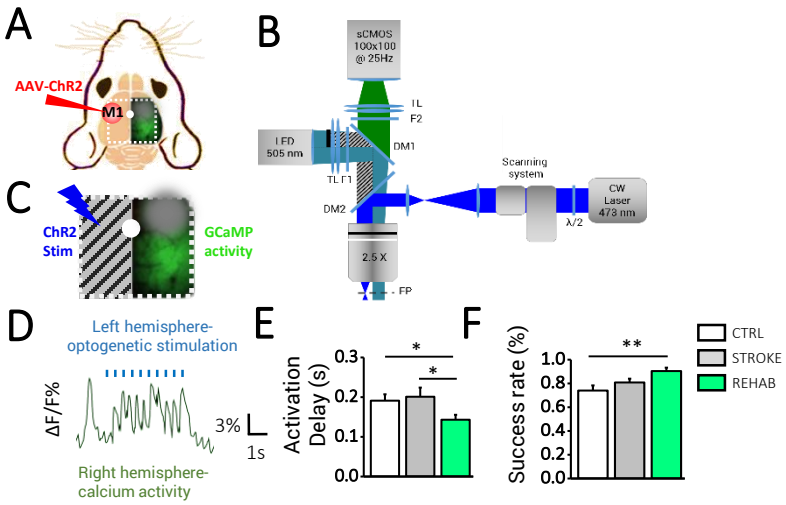

Figure 2: **All-optical stimulation and recording reveals strenghtened interhemispheric connectivity.** (A) Schematic representation of field of view (area within white dotted square) for all-optical investigation of inter-hemispheric functional connectivity on GCaMP6f mice. Red spot indicates M1 transfected with AAV-ChR2-mCherry; grey cloud highlights the site of the stroke lesion. White dot indicates bregma. (B) Wide-field microscope with double illumination path allowing simultaneous light stimulation and fluorescent recording. The inset on the top right highlights the hemi-occlusion of the illumination path to avoid spurious ChR2 stimulation. (C) The panel shows the simultaneous ChR2 laser-stimulation on the left hemisphere (not illuminated by LED light) and detection of the evoked fluorescence on the right side. (D) Fluorescent trace of optogenetically-elicited calcium activity. (E) Delay between delivery of laser stimulus and peak of the contralateral activation (average ± SEM; ANOVA post hoc Fisher, $P < 0.05$ for all comparisons; $Nmice_{CTRL} = 4$; $Nmice_{STROKE} = 3$; $Nmice_{REHAB} = 3$). (F) Success rate of laser-stimulation (average ± SEM, ANOVA post hoc Bonferroni $P < 0.01$).

Figure 3

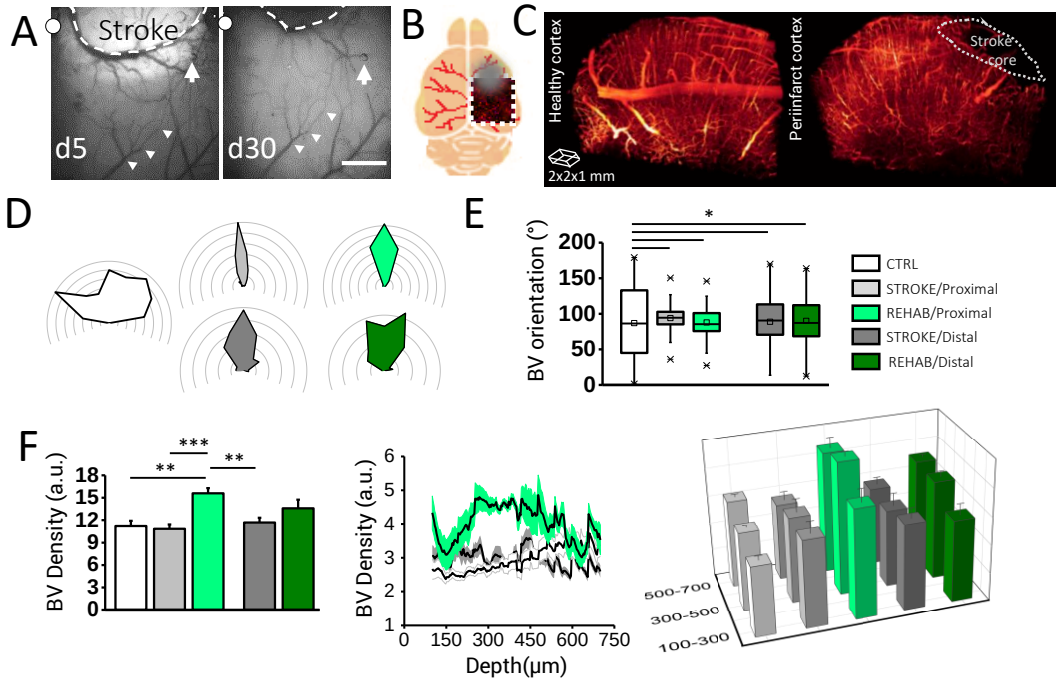

Figure 3: **Rehabilitation promotes angiogenesis in the peri-infarct area**. (A) Brightfield images showing cortical vasculature. The dotted line emphasises the profile of a big blood vessel shifting towards the core from 5 days to 30 days after stroke; similar translation is highlighted by the white arrowheads on a blood vessel distal from the injury site. The white arrow points at an internal reference on the image. White dots indicate bregma. (B) Schematic representation of fixed brain of GFPM mice, where vasculature is labeled with albumin-FITC (red lines). Dotted square highlights the imaged area; grey cloud indicates the stroke location. (C) 3D meso-scale reconstruction of vasculature in the controlesional healthy cortex (left) and in the peri-infarct area (right) from TDE-cleared cortical slice. The white dotted region highlights the absence of blood vessels in the infarct core. (D) The polar plot shows the distribution of blood vessels orientation in proximal and distal regions from the core for each experimental class (Nmice$_{CTRL}$ = 3; Nmice$_{STROKE}$ = 3; Nmice$_{REHAB}$ = 3). **The plots are oriented as in Fig. 3a, where lesioned area is on the vertical axis.** (E) The box plot shows the higher dispersion of angular distribution of the CTRL group compared to proximal and distal regions of all injured mice (Homogeneity of variance test, all variances significantly different from CTRL). (F) Blood vessel density analysis. *(Left)* The histogram shows the blood vessels density (average ± SEM) in proximal and distal regions (ANOVA one way, Bonferroni post-hoc test, *P* (REHAB Proximal/STROKE Proximal)<0.001, *P* (REHAB Proximal/CTRL)<0.01, *P* (STROKE Distal/REHAB Proximal)<0.01). *(Middle)* The graphs displays the blood vessels density profile with respect to brain cortex depth. Grey shadows report the SEM. *(Right)* 3D graph comparing average BV density grouped by cortical depths (300-500 µm from stroke core: *P*(REHAB Proximal/STROKE Proximal)<0.05; *P*(REHAB Proximal/STROKE Distal)<0.05; *P*(REHAB Proximal/CTRL)<0.05; 500-700 µm from stroke core: *P*(REHAB Proximal/STROKE Proximal)<0.05; *P*(REHAB Proximal/STROKE Distal)<0.05; ANOVA one way, Bonferroni post-hoc test).

Figure 4

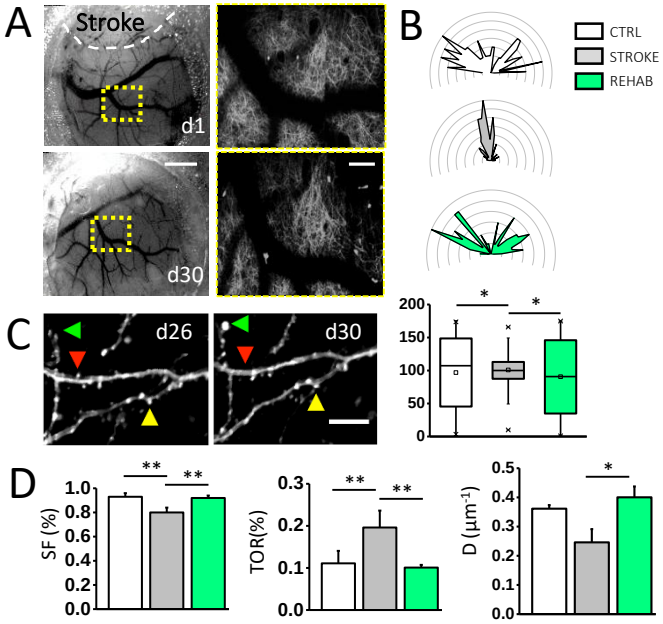

Figure 4: **Rehabilitation molds dendritic orientation and stabilizes spine turnover.** (A) Brightfield images showing vasculature under the cranial window one day and 30 days after stroke. The dotted yellow square highligts the rostral shift of a big blood vessel branching point due to damage, shrinkage of dead tissue and following displacement of perilesional cortical tissue. Scale bar, 1 mm. Right panels show the stitched two-photon images (4x4 MIPs of 130x130x50 μm^3) acquired within the region framed by the respective yellow squares in the left panels. Scale bar, 100 µm. (B) Polar plot showing the angular distribution of dendrites in the peri-infarct area. The plots are oriented as in Fig. 4a, where lesioned area is on the vertical axis. The box plot below shows the higher dispersion of the REHAB group distribution. (Homogeneity of variance test, $P<0.05$ for all comparisons; $Nmice_{CTRL} = 6$; $Nmice_{STROKE} = 4$; $Nmice_{REHAB} = 3$). (C) MIPs of two-photon stacks (z depth 8 µm) of dendritic branches 26 and 30 days after stroke respectively. The arrows point at a newly-formed (green), lost (red), and stable (yellow) spine. Scale bar, 5 µm. (D) The histograms show Surviving Fraction (SF) ± SEM (*left;* t-test, $P< 0.01$ for all comparisons), the Tournover Ratio (TOR) ± SEM (*middle,* t-test, $P< 0.01$ for all comparisons) and Density (D) ± SEM (*right panel,* t-test, $P< 0.05$) of spines in the peri-infarct area.

Supplementary Figure 1

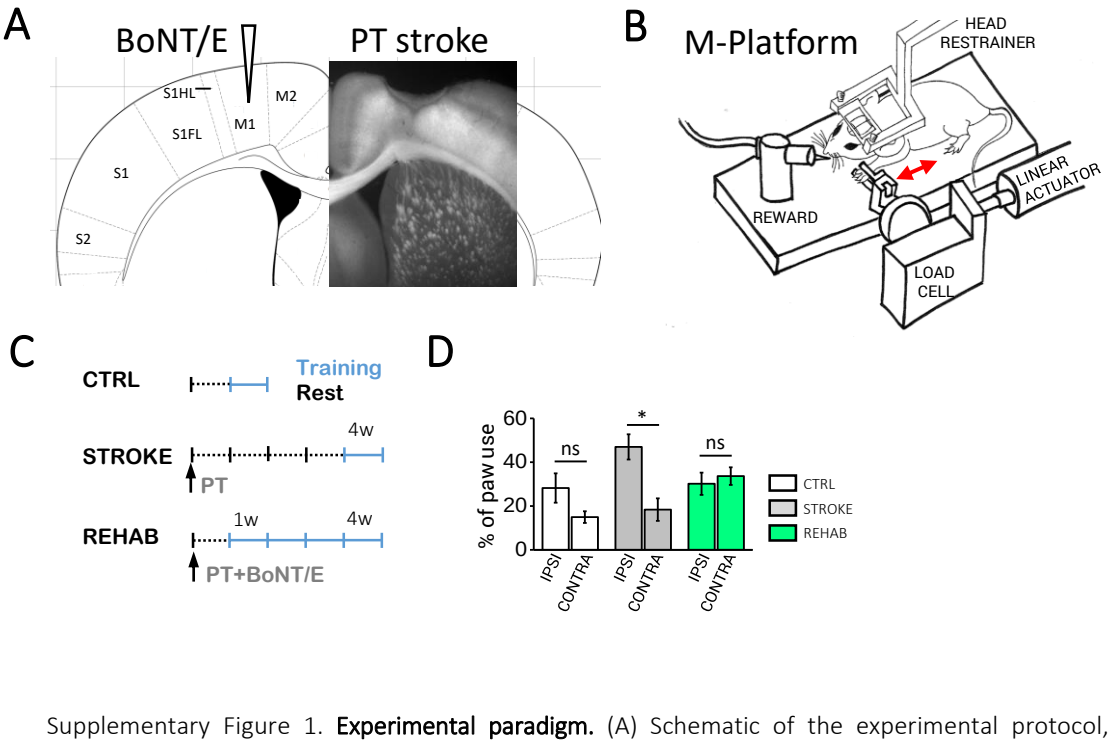

Supplementary Figure 1. **Experimental paradigm.** (A) Schematic of the experimental protocol, that combines photothrombotic stroke in primary motor cortex (M1) with contralesional injection of BoNT/E in the homotopic cortex. (B) Graphic representation of the M-Platform for rehabilitative training. (C) Experimental timeline for the CTRL, STROKE and REHAB groups in the awake imaging experiment. Light blue and dotted black lines refer to training and no-training weeks, respectively. W = week; PT = photothrombosis. (D) Histogram showing the % of paw use in the Schallert cylinder test performed by healthy 30 days post stroke (t-test ***P*** **(**IPSI/CONTRA STROKE)**<0.05**). IPSI and CONTRA refers to ipsilesional and contralesional paw, respectively; ns, non significant.

Supplementary Figure 2

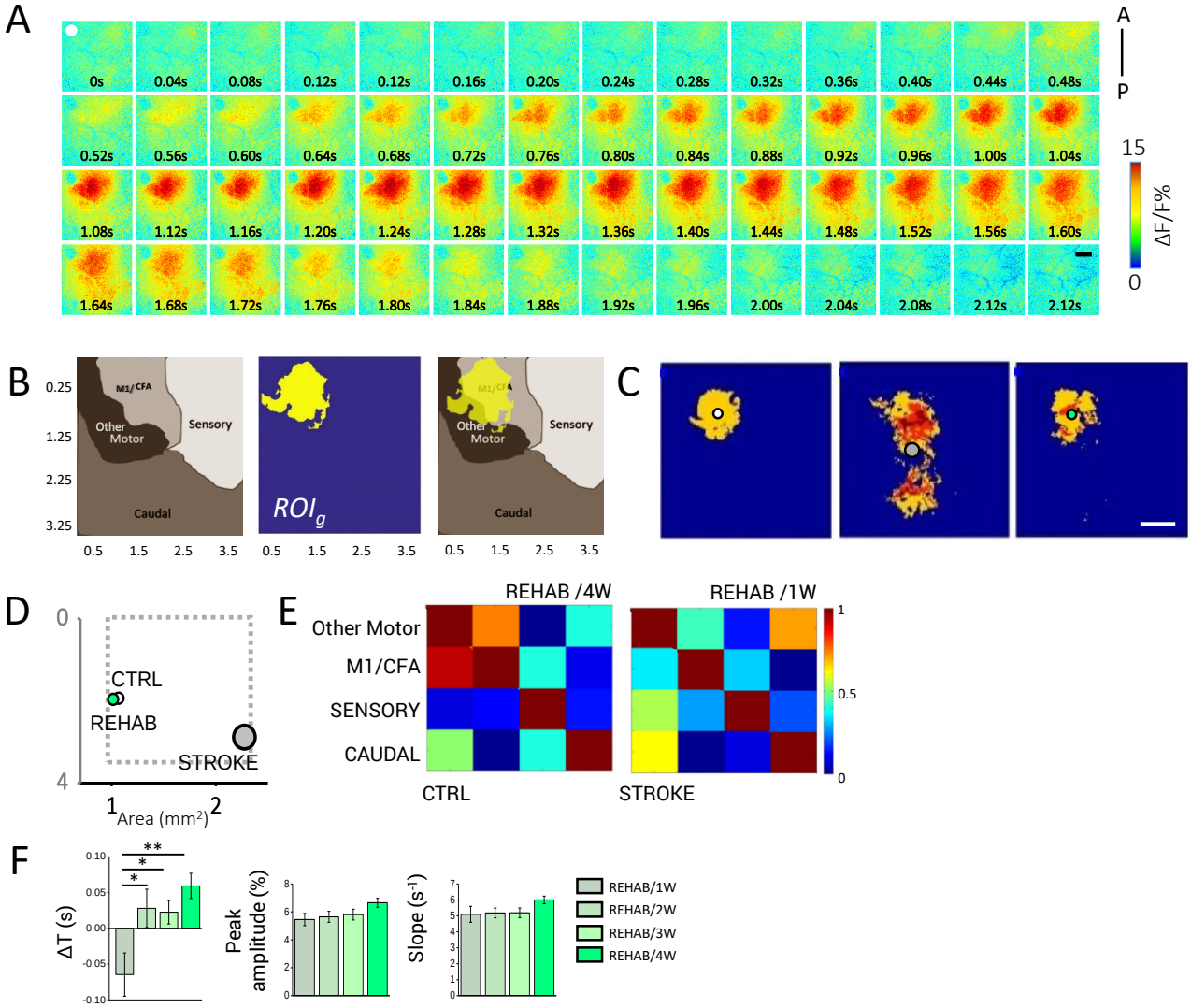

Supplementary Figure 2: (A) Complete image sequence of cortical activation during pulling of the handle by contralateral forelimb of a healthy GCaMP6f mouse. A-P, anterior-posterior. The white dot indicates bregma. Scale bar, 1mm (B) On the left, functional map based on ICMS studied of Tennant (2011, Cerebral Cortex) and Alia (2016, Sci Reports) used as reference maps. The middle panel shows the average thresholded ROI (ROI_g) computed for CTRL animals during voluntary pulling. On the right, merge of functional map and *ROIg*. CFA, Caudal Forelimb Area. Caudal area includes visual and associative regions. (C) The panels show the average thresholded ROI (ROI_g) computed for the different experimental groups. The circles represent the centroids of the ROI_g for CTRL (white), STROKE (gray) and REHAB (green) groups. (D) The Areas of the ROI_g and their distance from Bregma are reported into the scatter plot. REHAB mice are evaluated one week (REHAB/1W) and four weeks (REHAB/4W) after stroke. (E) Examples of partial correlation matrices of cortical activation during voluntary pulling. (F) **Left panel: Delays in cortical activation in caudal regions are reported for the 4 weeks of rehabilitative training (ANOVA One Way followed by Tukey Test, *P* (REHAB/1W-REHAB/4W)<0.01, *P* (REHAB/1W-REHAB/2W)<0.05, *P* (REHAB/1W-REHAB/3W)<0.05). Middle panel: maximum of fluorescence peaks for the 4 weeks of rehabilitative training. Right panel: The graph shows the slope (average ± SEM) of the fluorescence in the rising phase.** Unless otherwise stated, scale bar 1mm.

Supplementary Figure 3

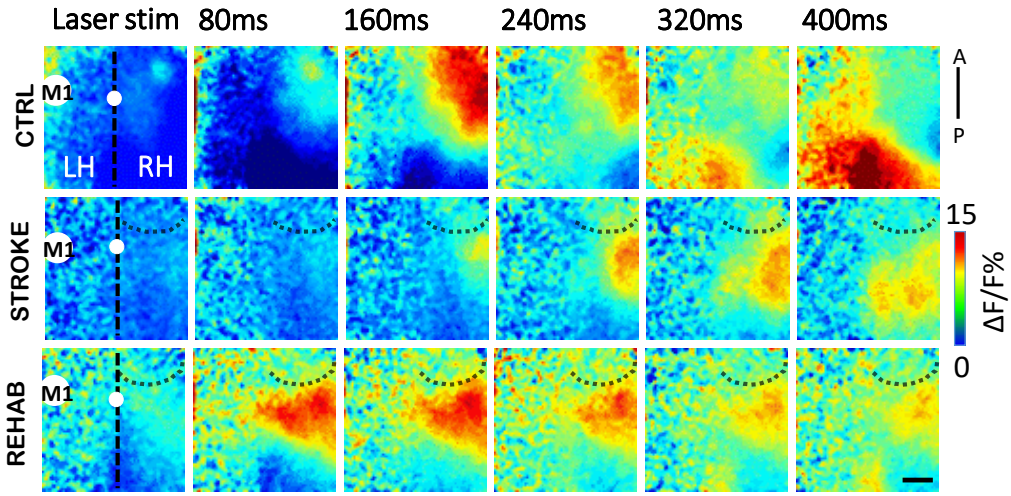

Supplementary Figure 3: Image sequences of ipsilesional cortical activation following laser stimulation on healthy M1. White spot on the black dotted line (midline) indicates bregma. A,P: anterior, posterior. LH, left hemisphere; RH, right hemisphere. Scale bar, 1mm.

Supplementary Figure 4

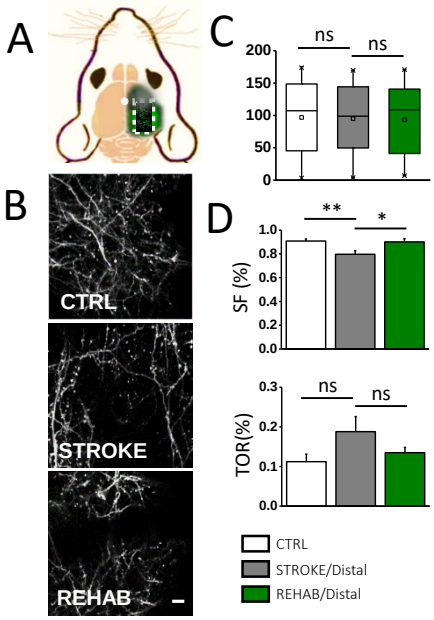

Supplementary Figure 4: (A) Schematic representation of field of view (i.e. area within white dotted square) of two-photon imaging of dendritic and spine plasticity on GFPM mice. Red spot indicates the site of the stroke lesion. (B) Examples of dendritic branches orientation in the peri-infarct area of CTRL, STROKE and REHAB group. Maximum intensity projection of two-photons stacks. Scale bar, 10 µm. (C) The box plot shows similar angular dispersion of dendrites in distal regions from the core for both the STROKE and the REHAB group distribution. (Homogeneity of variance test; ns, not significant). (D) The histograms show Surviving Fraction (SF) ± SEM (*upper panel;* ANOVA one way, Bonferroni post-hoc test, *P*(CTRL/STROKE Distal)<0.01, *P*(REHAB Distal/STROKE Distal)<0.05), the Tournover Ratio (TOR) ± SEM (*lower panel,* ANOVA one way, Bonferroni post-hoc test, not significant for all comparisons) of spines in the distal region (>1000 µm from stroke core).